Saudi Pharmaceutical Journal 29 (2021) 1070–1081

Contents lists available at ScienceDirect

Saudi Pharmaceutical Journal

journal homepage: www.sciencedirect.com

Original article

Formulation development and evaluation of lidocaine hydrochloride loaded in chitosan-pectin-hyaluronic acid polyelectrolyte complex for dry socket treatment

Nuttawut Supachawaroj [a,b,1], Teerasak Damrongrungruang [c,2], Sucharat Limsitthichaikoon [a,1,*]

[a] Department of Pharmaceutical Technology, College of Pharmacy, Rangsit University, Thailand
[b] Department of Oral Surgery, College of Dental Medicine, Rangsit University, Thailand
[c] Division of Oral Diagnosis, Department of Oral Biomedical Science, Faculty of Dentistry, Khon Kaen University, Thailand

ARTICLE INFO

Article history:
Received 4 March 2021
Accepted 4 July 2021
Available online 19 July 2021

Keyword:
3^2 factorial design
Dry socket treatment
Hyaluronic acid
Lidocaine hydrochloride
Polyelectrolyte complex

ABSTRACT

The main purpose of this study was to assess a lidocaine hydrochloride-loaded chitosan-pectin-hyaluronic polyelectrolyte complex for rapid onset and sustained release in dry socket wound treatment. Nine formulations (LCs) of lidocaine hydrochloride (LH) loaded into a chitosan–pectin–hyaluronic polyelectrolyte complex (PEC) were assessed using full factorial design (two factors × three levels). The formulations ranged between 4 and 10% w/w LH and 0.5–1.5% w/w HA. The following physicochemical properties of LCs were characterized: size, zeta potential, % entrapment efficiency, viscosity, mucoadhesiveness, % drug release, morphology, storage stability, and cytotoxicity. The particle size, zeta potential, % EE, viscosity, and % mucoadhesion increased with increasing LH and HA concentrations. Rapid release of LH followed a zero-order model, and a steady-state percentage of the drug was released over 4 h. LCs were found to be non-cytotoxic compared to LH solution. LH loaded into PEC demonstrated appropriate characteristics—including suitable rate of release—and fit a zero-order model. Furthermore, it was not cytotoxic and showed good stability in a high-HA formula, making it a promising candidate for future topical oral formulations.

1. Introduction

Dry socket, or alveolar osteitis, is the most common complication after tooth extraction and surgical removal of the wisdom tooth (Tarakji et al., 2015; Shevel, 2018). Dry socket pain starts one to three days after extraction or surgical removal of a wisdom tooth and usually presents with metallic dysgeusia and halitosis (Shevel, 2018). The pain (which can be 7–10 on the pain scale) is a significant problem in dry socket patients (Kamal et al., 2020), requiring administration of a topical analgesic (Metin et al., 2006). The primary objective for dry socket treatment is to attenuate the pain severity until sufficient epithelium granulation occurs to cover bone and nerve. The epithelialization time is variable but may be completed within 5 to 10 days (Veale, 2015). Thus, pain remedies should relieve acute pain (within minutes) and be released over a prolonged period for pain reduction until the re-epithelialization (or wound healing process) is completed.

Lidocaine hydrochloride (LH) has long been used as a topical dental anesthetic. The onset of LH is rapid, 1 to 2 min, and it reaches its highest efficacy within 5 min (Lee, 2016). Lidocaine is widely used in dental clinics and is available over-the-counter at a concentration of approximately 2–10% w/v in solution, gel, ointment, and spray forms. The incidence of a true allergic reaction to local lidocaine anesthetic is <1%, suggesting it is safe. Lidocaine and

Abbreviations: HA, hyaluronic acid; LC, lidocaine hydrochloride loaded in chitosan-pectin-hyaluronic acid polyelectrolyte complex; LH, lidocaine hydrochloride; PDI, polydispersion index; PEC, Chitosan-Pectin- Hyaluronic acid Polyelectrolyte Complex; Zn, zinc sulphate.

* Corresponding author at: Department of Pharmaceutical Technology, College of Pharmacy, Rangsit University, Pathumthani 12000, Thailand.
E-mail addresses: nuttawut.s@rsu.ac.th (N. Supachawaroj), dteera@kku.ac.th (T. Damrongrungruang), sucharat.l@rsu.ac.th (S. Limsitthichaikoon).
[1] Contact address: Department of Pharmaceutical Technology, College of Pharmacy, Rangsit University, Pathumthani 12000, Thailand.
[2] Contact address: Laser in Dentistry Research Group and Department of Oral Diagnosis, Faculty of Dentistry, Khon Kaen University, 40002, Thailand.

Peer review under responsibility of King Saud University.

Production and hosting by Elsevier

https://doi.org/10.1016/j.jsps.2021.07.007
1319-0164/

benzocaine are equally effective in attenuating pain from needle insertion relative to placebo (Garg et al., 2016).

Chitosan, a cationic polymer which possesses positive charge as a result of primary amine functional groups, is widely used for its biocompatibility and biodegradability (Das et al., 2011). Pectin has become popular as a natural, non-toxic anionic polymer (Das et al., 2011). Chitosan and pectin form complexes via the interaction of positive and negative charges (Folchman-Wagner et al., 2017), which, when combined with a drug of interest, can provide fast onset and sustained release of the drug (Mitrevej et al., 2001).

Hyaluronic acid (HA) is a component of the extracellular matrix of high molecular weight glycosaminoglycan. HA is biocompatible and offers anti-inflammatory, bacteriostatic, anti-edematous, and antioxidative effects (Dahiya and Kamal, 2014). In oral wound healing, HA, also known as hyaluronan, promotes cell proliferation, migration of matrix cells into the granulation tissue matrix, and granulation tissue organization (Deed et al., 1997).

Polyelectrolyte complexes (PEC) are self-assembling nanoparticles produced by electrostatic interactions between oppositely charged polyanions and polycations (Scheme 1) (Archana et al., 2013; Nath et al., 2015; Limsitthichaikoon and Sinsuebpol, 2019). Electrostatic interactions between oppositely charged macromolecules result in diverse structures and properties; for example, spherical or wormlike micelles, and hydrogels (Priftis et al., 2014). Under suitable conditions, the complexation from oppositely charged polymers, either binary or ternary system, in defined aqueous ratio can lead to form complex phase equilibria interaction (Scheme 1) (Priftis et al., 2014). The different types of PEC depended on the crossing interaction such as polymeric charges, proteins, surfactants, drugs (Marudova et al., 2004) and the preparation factors such as mixing ratio, mixing order, mixing time, and pH (Maciel et al., 2015; Potaś et al., 2020). Many natural polysaccharides are excellent polyelectrolytes and controlled-release carriers, providing nanometer-sized, efficacious enhancers. Polyelectrolyte complexes are emerging as promising vehicles for drug delivery to target sites, controlling the rate of drug release by carriers and prolonging the therapeutic activity (Naidu et al., 2009). Chitosan and pectin are natural polysaccharides that have shown potential in nanoparticle delivery systems (Wang et al., 2017). Since neither organic solvents nor chemical cross-linking agents are necessary for the PEC technique, possible toxicity and unfavorable side effects are reduced (Naidu et al., 2009). Recent studies have been used PEC for target drug delivery and medical devices for topical skin and mucosal applications, according to the PEC properties including mucoadhesion, swelling capacity, biocompatibility, and biodegradability (Ishihara et al., 2019; Potaś et al., 2020). Apart from the types of polyanion and polycation used, technical factors, such as pH alterations, charges density, ratio of polymers, or mixing order and time, are subjected to modulate and controlled to develop desired physicochemical and biological properties of the PEC (Potaś et al., 2020).

The main purpose of this study was to investigate a lidocaine hydrochloride-loaded chitosan–pectin–hyaluronic polyelectrolyte complex for rapid onset and sustained release in dry socket wound treatment. Physicochemical properties such as particle size, poly dispersion index, zeta potential, morphology, mucoadhesiveness, entrapment efficiency, loading capacity, percentage of drug released, cytotoxicity, and storage stability were measured.

2. Materials and methods

2.1. Materials

Low molecular weight chitosan (MW = 50,000–190,000 Da, degree of deacetylation (DD) = 55–70%, pKa = 6.5, lot no. STBF8219V), high methoxy pectin from citrus peels (pKa = 3.5, lot no. SLBQ6929V), and type II mucin from the porcine stomach (lot no. SLCC7713) were purchased from Sigma-Aldrich®, USA. Lidocaine hydrochloride (LH), hyaluronic acid (HA, MW = 1.8–2.2 MDa), and zinc sulfate (Zn) were purchased from Aketong Chemipun, Thailand.

2.2. Experimental design

A three-level, two-factor full factorial design was used to statistically optimize concentrations of LH and HA loaded into a chitosan–pectin–polyelectrolyte complex, and experimental trials were performed for nine possible formulations (shown in Table 1). The concentration of LH (X1) and HA (X2) were chosen as independent variables, and the dependent variables were particle size in micrometers (μm) (Y1), zeta potential in mV (Y2), entrapment efficiency in % (Y3), and percentage drug release within 5 min (Y4).

2.3. Formulation development

Briefly, from our previous study, chitosan was dissolved in 1% v/v acetic acid overnight to form a chitosan solution. Pectin was dissolved in deionized water, and LH was added to the pectin solution. LH (4, 7, or 10% w/w) in 0.1% w/w of pectin solution was added drop-wise to 0.3% w/w of chitosan solution and homogenized at 400 rpm for 5 min, then 0.04% w/w of zinc sulfate solution was added under continuous homogenization for 5 min. HA (0.5, 1, or 1.5% w/w) was added under continuous homogenization at 10,000 rpm for 10 min. The solution was sonicated 10 min triplicate in ultrasonication bath, 15 min resting time between each ultrasonication session was set (30 min total time for sonication) and controlled temperature at 28–32 °C to form LH loaded into the chitosan–pectin–hyaluronic acid polyelectrolyte complex (LC). The nine formulations (LCs), varying in LH and HA concentration, are shown in Table 1.

2.4. Physicochemical characterization

2.4.1. Particle size, poly dispersion index (PDI), and zeta potential

article size, PDI, and zeta potential were measured using dynamic light scattering (DLS) in a nanoparticle size and zeta potential analyzer (NanoPlus®, DLS Model NanoPlus-3 Serial no. 409314, USA). Each LC formula was dispersed in distilled water which the dilution factor equal 6 before measurement.

2.4.2. Viscosity and mucoadhesion

Viscosity (Ƞ, cps) of the nine formulations were measured (n = 6) using a viscometer (Brookfield Model DV-II + viscometer; USA) at 100 rpm and room temperature. Mucoadhesiveness, a measure of the bond strength between the formulation and glycoproteins in mucus (Graça et al., 2018; da Silva et al., 2018), was determined by mixing the formulation with type II mucin from a porcine stomach and inverting the tube five times without shaking. Each formulation mixed with water instead of mucin was used as average viscosity (Ƞ) of the formulation. The viscosity of the mixtures of formula + mucin was measured at 100 rpm at 0, 15, 30, and 60 min without re-shaking the sample. The percentage mucoadhesiveness was calculated by the following Eq. (2):

$$\%\ \text{Mucoadhesiveness} = \frac{\text{average } \acute{E} \text{ of the mixture} - \text{average } \acute{E} \text{ of formulation}}{\text{average } \acute{E} \text{ of formulation}} \times 100\% \quad (1)$$

2.4.3. Entrapment efficiency (%EE) and drug loading capacity

Centrifugal filter tubes (Amicon® Ultra, molecular weight cutoff [MWCO] of 3 K Da, Merck Millipore Ltd., Ireland) containing 1 ml of

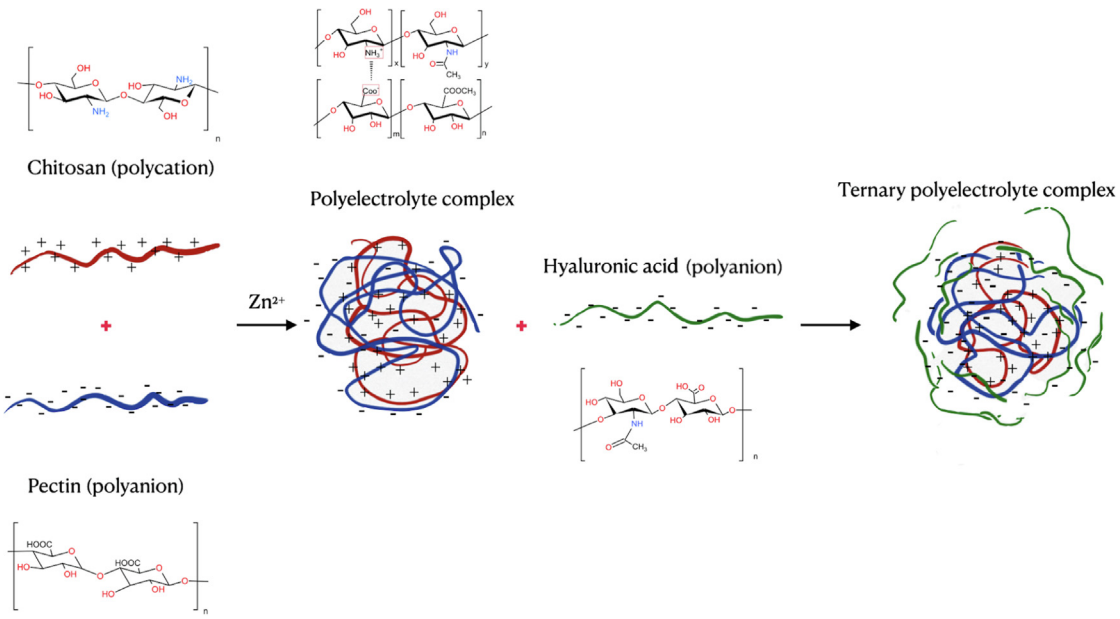

Scheme 1. Schematic Illustration of three different polymeric structures and ternary polyelectrolyte complex formation. The chemical structures of chitosan, pectin, hyaluronic acid, and polyelectrolyte complex were re-draw (Archana et al., 2013; Bukhari et al., 2018).

Table 1
2 factors 3 levels full factorial design for optimization of lidocaine hydrochloride (LH) and hyaluronic acid (HA) loaded in chitosan pectin polyelectrolyte complex.

Formulation	LH (%) (X1)	HA (%) (X2)	Viscosity (cps)	Size (μm) (Y1)	PDI	Zeta (mV) (Y2)	%EE (Y3)	%DL	%Drug releasing within 5 min (Y4)
LC1	4	0.5	5.4 ± 0.9	2.7 ± 0.9	0.544 ± 0.086	−7.2 ± 0.5	46.0 ± 0.3	4.33 ± 0.3	41.9 ± 0.4
LC2	7	0.5	8.8 ± 0.9	3.8 ± 2.0	0.519 ± 0.430	−10.0 ± 1.9	45.9 ± 0.7	4.32 ± 0.3	20.8 ± 0.8
LC3	10	0.5	14.4 ± 2.1	3.9 ± 0.6	0.337 ± 0.249	−13.2 ± 4.3	40.5 ± 0.4	3.89 ± 0.7	12.6 ± 0.5
LC4	4	1	26.8 ± 2.3	3.4 ± 1.2	0.004 ± 0.001	−22.8 ± 0.5	73.0 ± 0.1	6.83 ± 0.2	43.1 ± 0.1
LC5	7	1	32.0 ± 1.7	5.7 ± 3.2	0.139 ± 0.211	−22.3 ± 9.3	74.7 ± 0.0	6.70 ± 0.4	21.4 ± 0.2
LC6	10	1	57.0 ± 4.4	5.7 ± 0.7	0.122 ± 0.107	−25.0 ± 5.1	74.2 ± 0.2	6.93 ± 0.2	15.0 ± 0.1
LC7	4	1.5	177.2 ± 0.2	5.8 ± 0.9	0.127 ± 0.155	−27.7 ± 0.8	76.3 ± 0.4	7.18 ± 0.8	52.2 ± 0.2
LC8	7	1.5	228.8 ± 4.2	6.2 ± 1.1	0.006 ± 0.011	−21.1 ± 0.1	86.7 ± 0.0	8.19 ± 0.3	24.0 ± 0.1
LC9	10	1.5	287.2 ± 4.5	6.3 ± 0.5	0.004 ± 0.003	−22.6 ± 1.0	92.3 ± 0.1	8.71 ± 0.6	15.8 ± 0.2

each LC formula was centrifuged at 12,000 rpm for 30 min at room temperature. The supernatant solution was used to determine drug concentration using an ultraviolet (UV) spectrophotometer (Shimadzu UV1700; Japan) at 270 nm. Percent entrapment efficiency (% EE) and percent drug loading capacity (%DL) were calculated by the following Eqs. (2) and (3)

$$\%EE = \frac{\text{amount of total LH} - \text{amount of free LH}}{\text{amount of total LH}} \times 100\% \quad (2)$$

$$\%DL = \frac{\text{amount of total LH} - \text{amount of free LH}}{\text{amount of LH ternary polyelectrolyte complex}} \times 100\% \quad (3)$$

2.4.4. Microscopic morphology

The optimized formulations LC5 and LC8 were chosen to represent each group's morphology due to the formulation's stability, the concentration of HA, and the variability in parameters such as particle size, zeta potential, %EE, and %drug release.

Surface morphology and composition of LC samples were analyzed by scanning electron microscopy (SEM, FEI Quanta 450 Field Emission Scanning Electron Microscope, Austria). LC samples were pretreated by four-fold dilution with DI water sonicated for 5 mins, then mounted on a stub, gold-coated, and observed at 30,000× magnification.

The LC samples' morphological characteristics were observed by transmission electron microscopy (TEM, FEI Company, USA). TEM was observed at 10,000–20,000× magnification after a drop of each four-fold diluted sample was applied to a copper grid coated with carbon film and air-dried.

2.5. In vitro drug release

Approximately 5 g of LC samples, contained LH of 4, 7, and 10 % w/w in each ratio of the formulation, were placed in a dialysis bag (dialysis membrane standard RC Tubing MWCO 3.5 K Da, Spectra/Por®, USA), avoiding the gas bubble and embedding the sample in the receptor chamber containing artificial saliva solution (pH = 7.4). During the entire experiment, the receptor chamber was held in a shaking water bath using magnetic clips at 37 ± 2 °C and stirred at 600 rpm. At 5, 10, 15, 30, 60, 120, 240, 480, 720, and 1440 min, 5 ml of the receptor medium was collected and replaced with fresh receptor medium. Each sample was then collected from the receptor media and analyzed for LH percentage at a wavelength of 270 nm. Cumulative total LH permeated from each sample was calculated as a percentage of its donor's total LH content.

2.6. Stability study

All LC formulas were stored in a desiccator for 3 months at room temperature to determine their stability. After 3 months of storage,

the physical properties of the nine formulations were analyzed and their zeta potential was determined.

2.7. Cell viability

The effect of the LC formulation on cell viability was determined using human gingival fibroblasts (HGF-1, ATCC®, CRL-2014™, USA). HGF-1 were cultured in high-glucose DMEM supplemented with 1% antibiotic–antimycotic (containing 100 U/mL of penicillin, 100 μg/mL of streptomycin, and 25 μg/mL amphotericin B; Invitrogen, USA) and 10% v/v fetal bovine serum (FBS; Gibco, USA) in a humidified incubator (Thermo Fisher Scientific™, USA) at 5% CO_2 and 37 °C. The HGF-1 was prepared for the MTT assay by seeding 20,000 cells/well in 96-well plates in an FBS-free medium solution. The cells were then exposed to LC3, LC6, LC9 and LH (concentration varied between 50 and 1000 μg/ml) and incubated in a humidified incubator (5% CO_2, 37 ± 1 °C, 90% relative humidity) for 24 h. The percentage of cell viability was analyzed using the MTT method, which was calculated by the absorbance of the sample compared to the absorbance of the negative control (using DMEM solution and blank niosomes) in the same culture plate, following Eq. (3):

$$\text{Percentage of cell viability} = \frac{\text{Average absorbance of sample}}{\text{Average absorbance of negative control}} \times 100 \quad (4)$$

2.8. Statistical analysis

Categorical variable data were estimated into percentages or ratios (all n = 6, except n = 8 in cell viability test). Continuous variable data were reported as means and standard deviations (SD) and the normality was tested. Student *t*-test and analysis of variance (ANOVA) were performed to test differences between or among experimental groups using SPSS 13 software (SPSS Inc, Chicago, IL, USA). The 3^2 full factorial experiment was designed using Design-Expert® v.11.0.3 (Stat-Ease, Inc., Minneapolis, MN, USA). For statistical significance ($p < 0.05$), either a Student's *t*-test or ANOVA were used to compare the average values.

3. Results and discussion

3.1. Formulation development

In our previous study, PEC was investigated the complex forming through the interaction between positive charges of CS and negative charges of PC. The effects of pH and pKa of the polymeric solution were related to the physicochemical properties such as particle sizes, zeta potential, %drug loading and %drug entrapment. Moreover, the result on increasing of CS concentration obtained large size of the particles and precipitation of the complex occurred. This flocculation might cause from the electrostatic imbalance of polyelectrolyte complex which these results also similar to the increasing of polyanion concentration as PC or HA. On the other hand, increasing double ratio of CS:PC as 6:2, 6:1, or 5:2 was found rapid aggregation of the polyelectrolyte system. Several studies of CS-PC polyelectrolyte complex provided the similar results of our experiments such as effects of the pH and pKa (Maciel et al., 2015) and mass ratio of polymers which affected to increase the particle sizes and decrease absolute zeta potential of the PEC system (Wang et al., 2017; Potaś et al., 2020). Thus, the ratio 3:1 of CS:PC was used to formulate ternary polyelectrolyte complex of CS-PC-HA.

Nine formulations of PEC composed of the positively charged chitosan and the negatively charged pectin with HA and LH were analyzed by a 3^2 full factorial design. The LH varied from 4 to 10% w/w and HA from 0.5 to 1.5% w/w according to the range of lidocaine and hyaluronic dose concentration.

3.2. Particle size, polydispersity index, and zeta potential

The LC particle sizes were in the range of 2.7–6.3 μm (Table 1 and Fig. 1a), in which a high concentration of HA groups (LCs 7–9) provided the largest sizes. The ternary complexes composed of chitosan, pectin, and hyaluronic acid was formed by the interaction of opposing charges and the electrostatic force of the amino ionic groups of chitosan (NH^{3+}), the carboxyl groups (COO^-) of pectin (Archana et al., 2013; Borges et al., 2015; Hong et al., 2018) and the hydroxyl group (OH^-) of hyaluronic (Nath et al., 2015; Bukhari et al., 2018). The anionic-cationic charge ratio of chitosan: pectin: hyaluronic results from the formation of a macromolecules polyelectrolyte complex (Priftis et al., 2014; Limsitthichaikoon and Sinsuebpol, 2019). Compared to the CS-PC binary polyelectrolyte complex, the present of HA significantly increased the particle sizes from nanosize range (400–600 nm) to micron scales (2–7 μm). The larger size of LCs 7, 8, and 9 might result from ternary PEC preparation, which influences the strength of electrostatic interaction (Zhang et al., 2016; Folchman-Wagner et al., 2017; Wang et al., 2017; Hong et al., 2018). Moreover, the PDI increased disproportionally with increasing particle size, demonstrating the particle size uniformity (Fig. 1a).

All the formulations provided the negative zeta potential value which were from the proportions of LH, HA, and pectin. The zeta potential of nine formulations were observed in a range of −7.2 to −27.7 mV, as shown in Fig. 1b. The lowest concentration of HA provided lowest zeta potential value which had absolute charge <13.2 mV. The formulation LC4–LC9 observed the zeta potentials of −21.1 to −27.7 mV. The zeta potential value of negative or positive charge that is <15 mV represents the beginnings of agglomeration of particles lead to less area of interaction with incoming substances or particles while the value above 16–30 mV is a threshold of delicate dispersion and lead to prompt interact with incoming substances or particles (Sherman, 1970; Lee, 1998). The LC4–LC9 provided absolute value of zeta potential of above −20 mV (Fig. 1b) could be represented the approximate stability of dispersion. Even though all LC formulations had zeta potentials lower than −30 mV, LC8, after three months of storage at room temperature, had a significantly greater zeta potential than freshly prepared ($p < 0.01$). The zeta potential of LC9 was not significantly different in stored and fresh samples ($p > 0.05$) (Fig. 1b). The particle size and zeta potential increased as the concentration of LH and HA increased. The HA concentration had a greater effect on size than LH due to HA's negative charge (Table 1), allowing it to form cross-links and possibly coat the particle (Gennari et al., 2019).

Forming suitable condition of the ternary PEC, ratio of chitosan: pectin: hyaluronic can lead to form complex phase equilibria interaction (Scheme 1) (Priftis et al., 2014). In which the LH concentration increased, and HA concentration was fixed, there was a significantly increase in particle size (Table 1). We obtained similar results when HA concentration was increased, while the concentration of LA was fixed. Although incorporating high concentration of HA significantly develops the large particle size, the present of HA, as ternary polymer in the CS-PC polyelectrolyte complexes, helps induced particle size stability (Hong et al., 2018) by reduced the PDI and increased zeta potential, viscosity, %EE and %DL.

3.3. Viscosity and mucoadhesiveness

The viscosity and mucoadhesiveness were greatest in formulation LC9, which had the highest LH and HA concentrations (Table 1

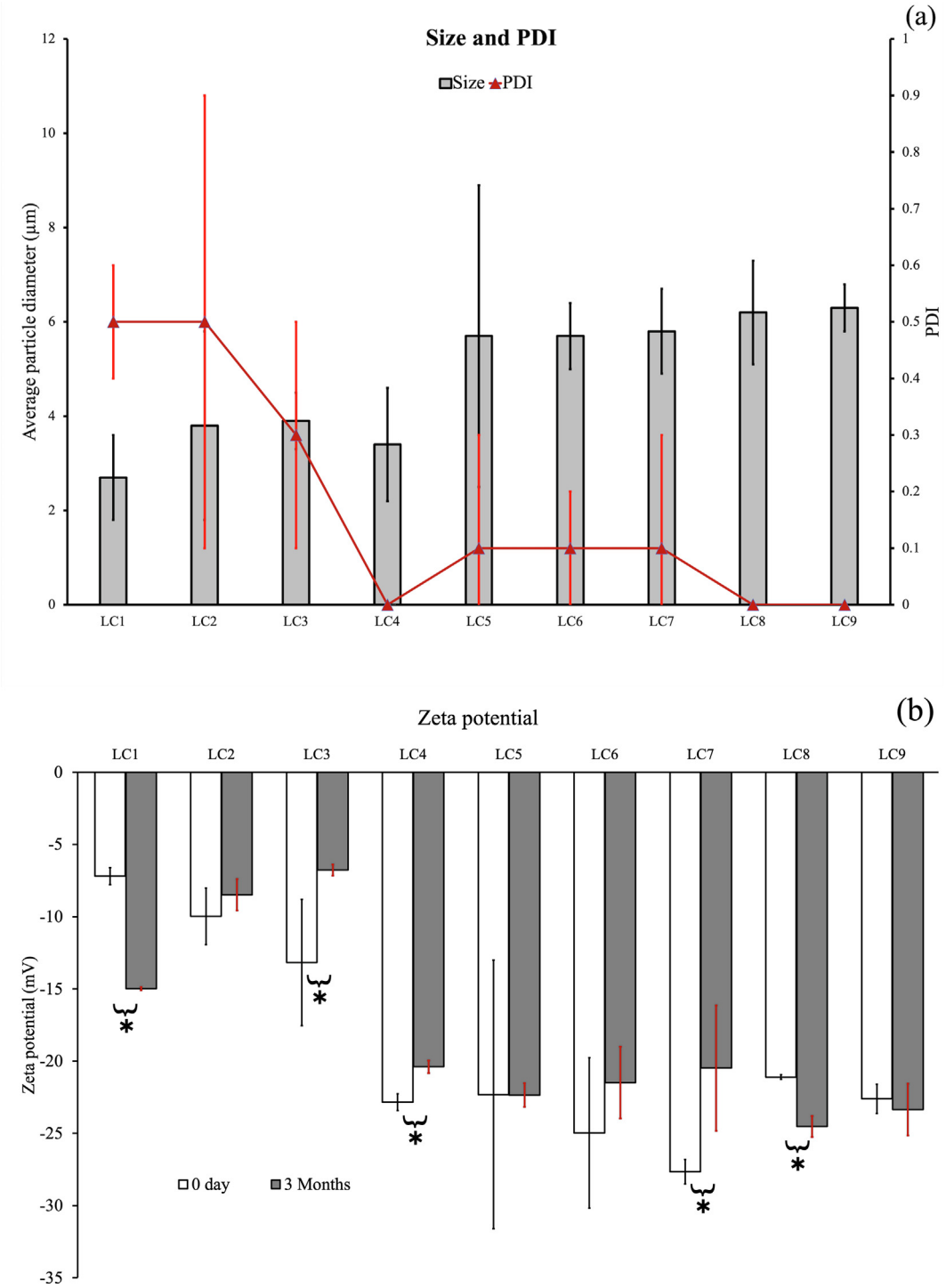

Fig. 1. The comparison between particle size (gray columns) and polydispersity index (PDI) (red dot) (a) and zeta potential of LC formulations varied using a 3^2 factorial design (b) in which white columns present the zeta potential of freshly prepared LC (day 0) and grey columns present zeta potential values after 3 months of LC storage at room temperature. Error bars show SD (n = 6); symbols indicate significant differences at $p < 0.05$: *compared to the freshly prepared and (3 months) stored LCs, using Student's *t*-test.

and Fig. 2a). The HA concentration had a greater effect than that of LH, as observed in the results of LC3, LC6, and LC9 formulations: viscosity increased four-fold from LC3 to LC6 and from LC6 to LC9. The main factor that influences LC viscosity is HA concentration. This might explain by the nature of this molecule which acts as a reservoir to entrap some certain factors in an extracellular matrix. The duration of formula-mucin interaction also affected % mucoadhesiveness (Fig. 2a). The % mucoadhesiveness was greatest at 15 mins and decreased after 30 and 60 min of bonding. The formula–mucin bond was, therefore, weak, possibly due to the hydrogen bonding between the hydroxyl and carboxyl groups (Graça et al., 2018). The ionic bond of the formula–mucin complex can be active, but the formula and mucin's negative charges allow for a weak bond that could decrease over time (Graça et al., 2018).

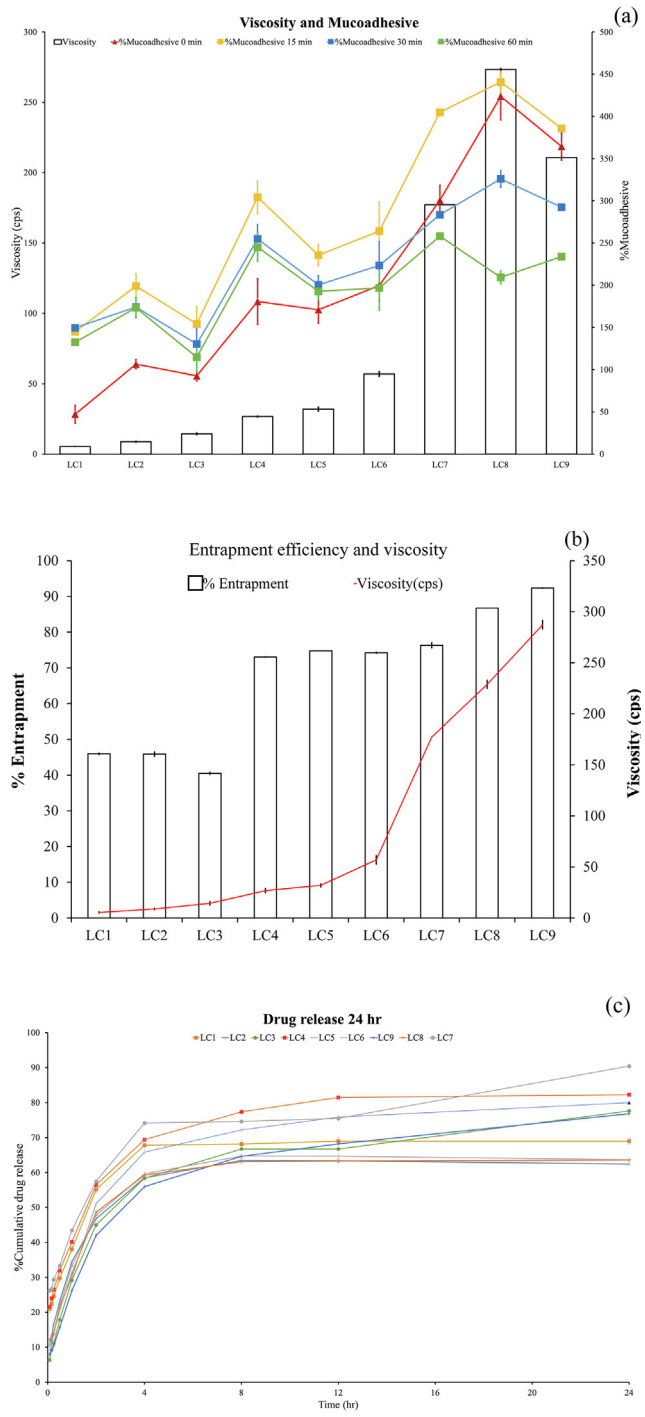

Fig. 2. Comparison of (a) the formulation viscosity (white columns) and **%** mucoadhesiveness at 0 (red line), 15 (yellow line), 30 (blue line) and 60 min (green line), (b) percentage of entrapment efficiency (white column) and viscosity of freshly prepared LC formulations (red line) and (c) percentage of cumulative drug-release of 9 formulations of LC varied in 3^2 factorial design at 24 h which data are average % cumulative amount ± SD (n = 6). Error bars represent standard deviations (SD) (n = 6).

Moreover, we observed external forces (or stimuli), such as vibration, made the formula–mucin interaction stronger. This result is likely important in formula application.

3.4. Entrapment efficiency and drug loading capacity

The ratio of LH and HA also affected the entrapment efficiency and drug loading capacity. In those formulations in which the LH concentration increased and HA concentration was fixed, there was a slight increase in entrapment and drug loading. And the same was true when HA concentration increased, and the concentration of LH was fixed. The increasing viscosity might be due to the entrapment of the LH inside the PEC, directly resulting in a high % EE and %DL formulation (Graça et al., 2018; da Silva et al., 2018).

3.5. Morphology

SEM photographs of all formulations (Fig. 3a and b) showed nanometer-sized particles (red arrowhead) dispersed on the polymeric micelle background (white arrowhead). Similarly, LCs observed via TEM (Fig. 3c and d) appear as sphere-like vesicles with nanometer-sized particles. The photographs of LC5 and LC8 showed the same morphology. However, the SEM- and TEM-based size estimates were not consistent with the results of DLS particle size analyses, which showed that these polymeric micelles surrounded the LC molecule and reflected the light, making it appear larger than the particles. The DLS method may not accurately represent polymeric micelles. Optical microscopy images and high magnifications of SEM or TEM may better describe particle morphology and micelle structure.

3.6. Drug release

The cumulative release of LH from LC was investigated *in vitro* over 5 min, 2 h, and 24 h. These time points were used to assess the dual-phase action of LC formulations for dry socket treatment, which requires the early-onset and prolonged release of pain reliever LH until re-epithelialization is complete (Burgoyne et al., 2010). Therefore, an LH burst effect is essential, and our goal is to provide initial drug release in 5 min.

At 5 min, the results of the burst effect (Table 1) showed that when comparing formulations with the same HA concentrations (low HA group LC1, LC2, and LC3; medium HA group LC4, LC5, and LC6; high HA group LC7, LC8, and LC9), the increased viscosity of the higher HA concentrations retarded drug release.

When the HA concentration was varied, the high release formulations were LC1, LC4, and LC7, the middle group included LC2, LC5, and LC8, and the low group included LC3, LC6, and LC9, which also correlated to HA concentration. Thus, HA concentration directly affected the percentage of LH release. Moreover, the burst effect of LH release also lowered % EE and viscosity.

From Table 2, in the initial 2 hr of LH release were examined using multiple kinetic models, zero-order is a model that plotted as cumulative amount of drug released and time (5), first-order is a model that plotted as log cumulative amount of drug released and time (6), and Higuchi is a model that plotted as cumulative amount of drug released and square root of time (7):

$$Q = k_0 t \quad (5)$$

$$\ln Q = \ln Q_0 - k_1 t \quad (6)$$

$$Q = k_H t^{1/2} \quad (7)$$

where Q is the amount of drug release at time, Q_0 is the initial drug concentration, k_0 is the rate constant corresponding to zero order model, k_1 is the rate constant corresponding to first order model, k_h is the rate constant corresponding to Higuchi order model, t is time in hour, and $t^{1/2}$ is the square root of time.

The profile of drug release within 2 h was analyzed by linear regression (Table 2), and each formula was fitted into zero-order, first-order, and Higuchi models (Mhlanga and Ray, 2015). LC release was best fitted to zero-order kinetics, as the r^2 approached 1, indicating that the LC formulations provided controlled delivery

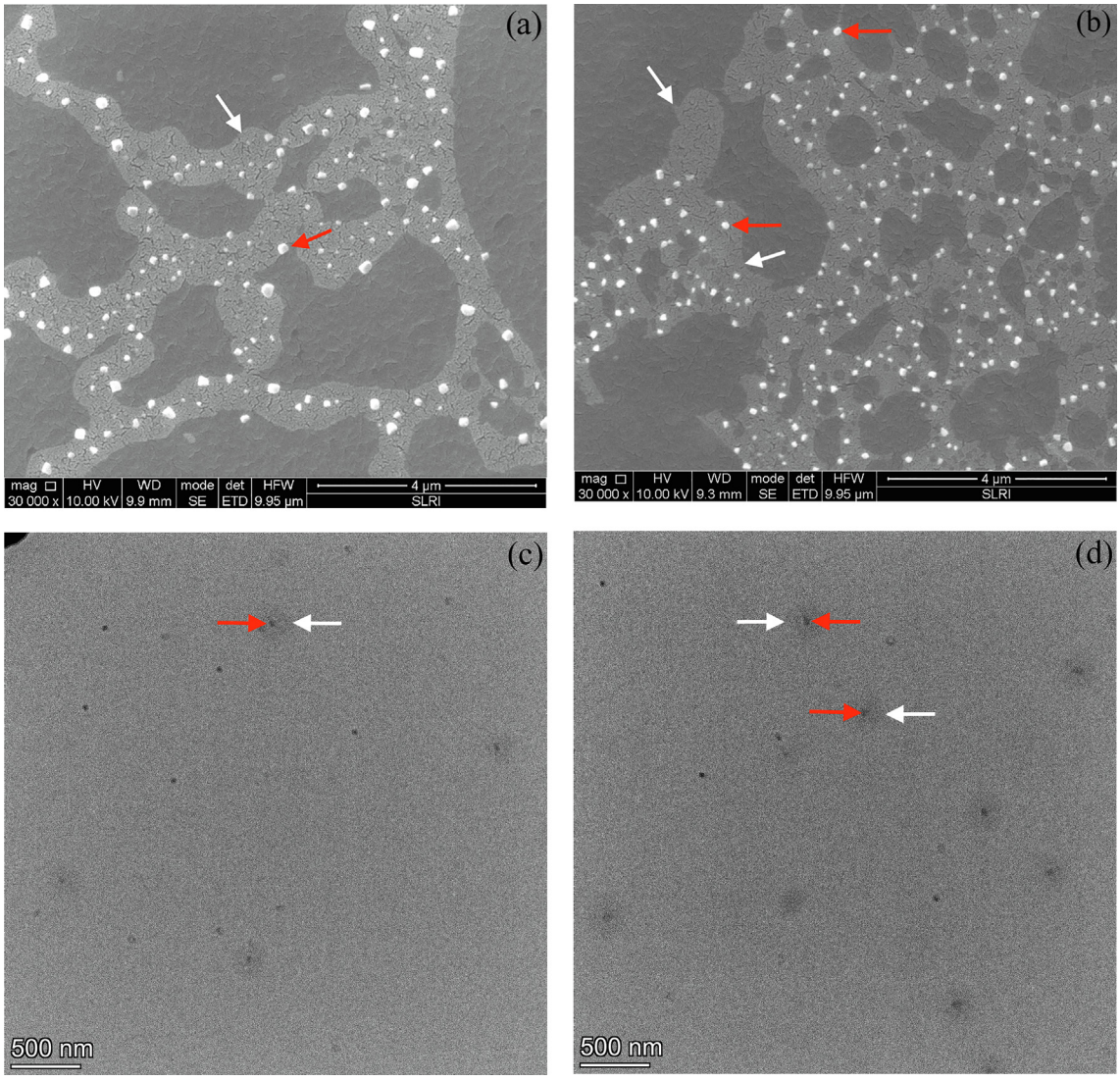

Fig. 3. Micrographs observed under scanning electron microscopy (SEM) of LC5 (a), LC8 (b) and transmission electron microscopy (TEM) of LC5 (c) and LC8 (d), at 25,000× magnification, showing molecular dispersions of LH in PEC form, between 50 and 100 nm. The red arrow indicates PEC particles, while the white arrows point to polymeric micelles.

Table 2
Drug release over 2 hr, during which the coefficient of correlation (r^2) demonstrated behaviors of zero-order, first-order, and Higuchi release models.

Formulation	Zero-order			First-order			Higuchi		
	r2	slope	Intercept	r2	slope	Intercept	r2	slope	Intercept
LD1	0.9982	35.488	39.973	0.9706	0.2154	1.6337	0.9781	60.892	19.808
LD2	0.9615	37.605	23.129	0.8593	0.3171	1.4112	0.9976	66.396	0.4129
LD3	0.9814	40.157	23.129	0.8726	0.4102	1.32238	0.9934	69.856	10.769
LD4	0.993	35.585	43.15	0.9533	0.2082	1.6618	0.9888	61.55	22.575
LD5	0.9781	39.648	19.924	0.8976	0.3396	1.3714	0.9901	69.146	3.4092
LD6	0.9889	43.803	15.815	0.8688	0.3878	1.3057	0.9869	75.853	9.575
LD7	0.993	33.373	49.871	0.9684	0.1816	1.7184	0.9803	57.477	30.753
LD8	0.9951	39.021	20.637	0.9427	0.3208	1.238	0.9766	67.005	1.5733
LD9	0.9961	36.218	13.028	0.9355	0.375	1.238	0.9765	62.159	7.5636

(Swain et al., 2019). Optimal duration of controlled drug release for dry socket management depends on the size of the exposed bone area, but it usually ranges from 5 to 10 days (Blum, 2002); the most painful period during dry socket occurs 2–3 days after the tooth is removed. Thus, rapid onset of pain reduction and pain control is needed until the wound is healed. Fig. 2c presents the percent cumulative LH release sustained after 4 hr and controlled within 24 hr for all formulations.

3.7. Stability analysis

The zeta potentials of LC formulations stored for 3 months were compared to the zeta potentials of freshly prepared formulations. The results show that 10 min after preparation, the low HA concentration formulations (LCs 1–3) began to separate and were completely separated within 30 min (Fig. 4b). Although they could be homogenized after shaking (Fig. 4a), they separated again within

10 min, indicating unstable formulations. Formulations with a zeta potential of approximately −20 mV or lower were more stable (Fig. 1b), aggregating faster than other groups (Ostolska and Wiśniewska, 2014; Raoufi et al., 2017).

After 3 months, co-aggregation and separation was observed in LCs 4–7, while LC8 and LC9 were homogeneous (Fig. 4c). The zeta potentials of the stored LC 4–7 formulations were less than those of the freshly prepared samples, implying these formulas are unstable (Ostolska and Wiśniewska, 2014; Raoufi et al., 2017). Viscosity also affected the formulation stability, and LCs 1–7 had a lower viscosity than LC8 and LC9 (Fig. 2b). The interacting colloidal forces' impact on the viscosity may affect repulsion energy. This phenomenon may be due to electrostatic repulsion and Van der Waals attraction retarding the Brownian movement of the colloidal system, resulting in precipitate protection (Genovese and Lozano, 2006; López-Esparza et al., 2015).

3.8. Optimization: Factorial analysis and validation

The dependent factors were A = lidocaine hydrochloride concentration and B = hyaluronic acid concentration. The independent factors (response parameters) were particle size, zeta potential, % entrapment efficiency, and % drug release within 5 min.

$$\text{Size} = 678.1A + 1312.11B + 4812.23 \quad (8)$$

(R^2 = 0.8668)

$$\text{Zeta} = 6.42B^2 - 1.94A^2 + 2.75AB - 6.84B - 0.51A - 22.07 \quad (9)$$

(R^2 = 0.9855)

$$\text{Entrapment efficiency} = -2.06A^2 - 9.4B^2 + 5.37AB + 1.96A + 20.49B + 75.41 \quad (10)$$

(R^2 = 0.9978)

Drug release at 5 min resulting from 3^2 full factorial design

$$\text{Drugrelease} = 8.24A^2 - 1.1B^2 - 1.76AB - 15.48A + 2.8B + 21.36 \quad (11)$$

(R^2 = 0.9910)

Concentrations of LH and HA significantly affected particle size, zeta potential, % EE, and drug release within 5 min ($p < 0.05$). Multiple regression analyses suggested a linear relationship between LH and HA concentrations and particle size, % EE, and drug release, while there was a quadratic relationship between concentration and zeta potential. The equations for particle size, zeta potential, % EE, and drug release are shown in Eqs. (8), (9), (10), and (11), respectively. The 3D response surface and contour plots demonstrating the effect of variables are shown in Fig. 5a, b, c, and d, respectively. These effects are probably attributable to two factors. First, the HA concentration increases the viscosity. HA, a hydrophilic polymer (Graça et al., 2018; Gennari et al., 2019), was the last component added to the formulation, and could expand to envelop the other components. It increased particle size and % EE and retarded drug release. Second, a high negative zeta potential may result from adding HA, an anionic polymer (Graça et al., 2018; Gennari et al., 2019). Therefore, increasing HA concentration directly increases the zeta potential.

The factorial design is an effective method for experiment to study effect of factors in small sample size, with cost-effectiveness, and lower time consumption. Three level full factorial design is a study to investigate about quadratic relationship between the response and each of the factors and of polyelectrolyte complex. Pandey et al., optimized 32 full factorial design of CS-PC polyelectrolyte complex for colon target drug delivery and demonstrated a success in drug releasing to colon (Pandey et al., 2013). Surprisingly, their ratio design of CS:PC was 3:1.1 which similar to our study and their results showed that in this ratio could yield the highest %swelling and %drug release at 12 h. Although our design investigated the interaction of LH and HA in the fixed ratio of CS:PC at 3:1, this intervention did not retard the %release rather the principle effect of %swelling and %drug release were derived from LH and HA.

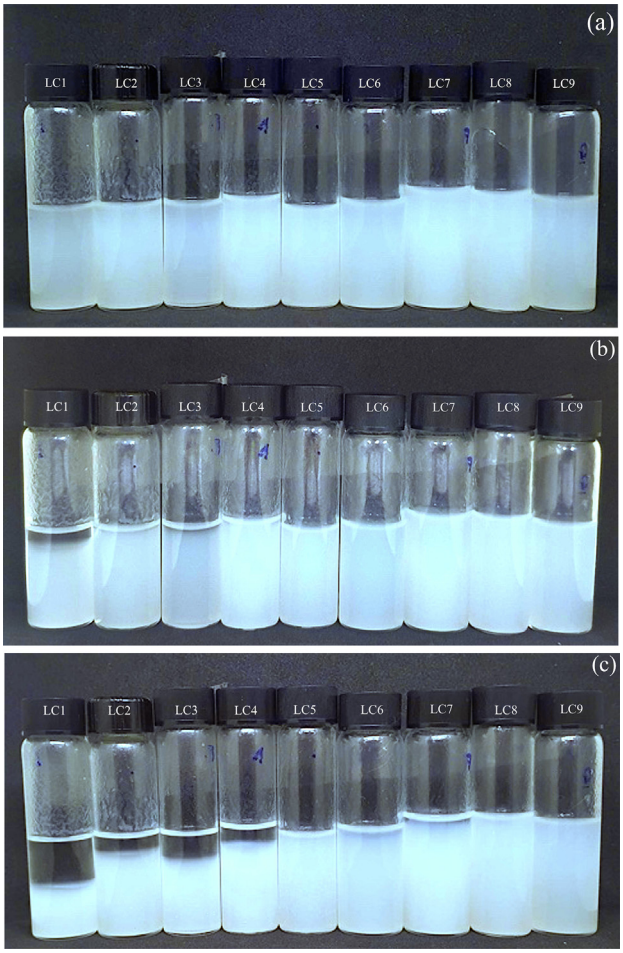

Fig. 4. Stability of LC1 to LC9 formulations at room temperature (a) freshly prepared, (b) 15 min after preparation, and (c) after 3 months of storage. Compared to freshly prepared, LC1–LC3 particles sedimented rapidly, within 15 mins after preparation, while LC4–LC7 were completely separated after 3 months of storage. LC8 and LC9 were homogenous solutions, indicated the stability of those PEC formulations.

3.9. Cell viability

The purpose of cell viability study is to observe the biocompatibility after composed LH loaded in the PEC and the cytotoxicity of each component. Even though each ingredient provides no cytotoxicity effect, after combined all of materials synergetic consequence or any toxicity caused from the interaction of the formulation might occur and needed to prove in *in vitro* cytotoxicity study. Cell proliferation, implied from cell viability, was determined for formulations with high LH and varied HA concentrations. The cell viability was evaluated to determine the effects of PEC loaded with 50–1000 μg/ml of LH (formulations LC3, LC6, and LC9) and different HA concentrations. HGF-1 cells were also used to test the cell viability for blank PEC, HA, and Zn. The results (Fig. 6a) showed that all other PECs besides LC3, LC6, and LC9 did not affect the cell viability. Compared to un-loaded

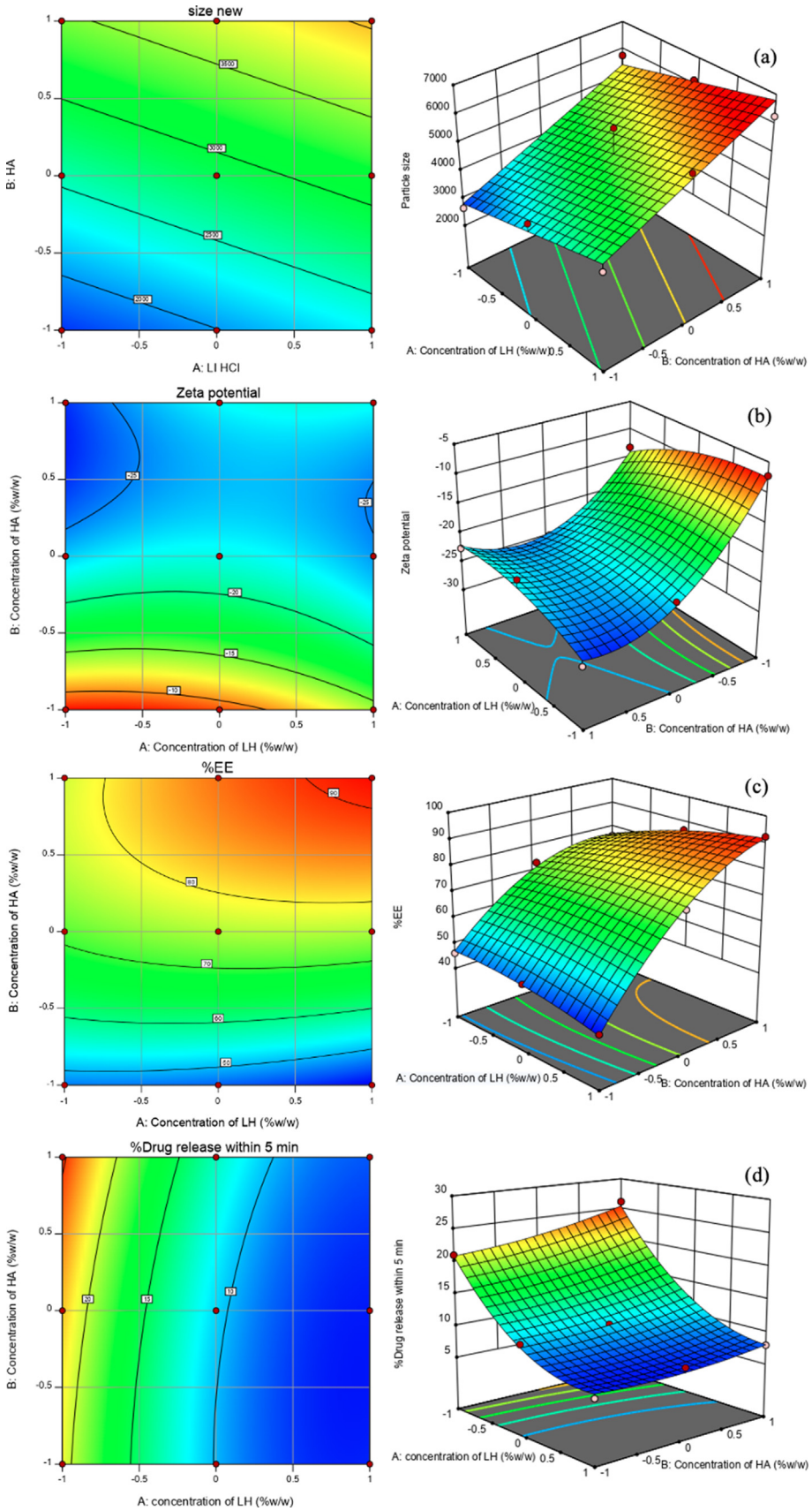

Fig. 5. Response surface plot and contour plot of independent variables LH (lidocaine hydrochloride) and HA (hyaluronic acid) on (a) particle size, (b) zeta potential, (c) entrapment efficiency, and (d) drug release at 5 min.

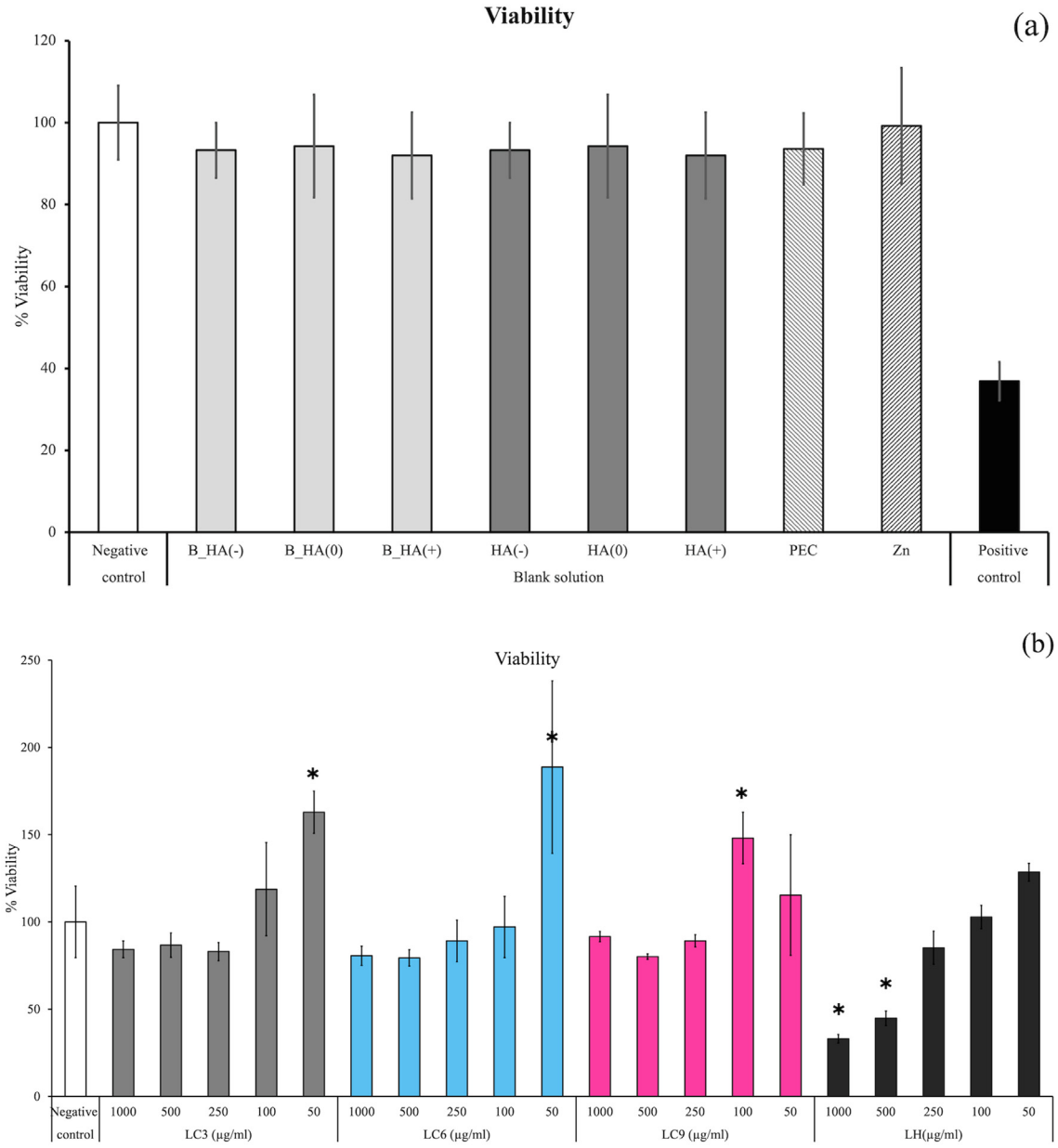

Fig. 6. HGF-1 cell viability by MTT assay (n = 8) at 24 h in blank DMEM as a negative control, HA (-), HA (0), HA (+), and DMEM with FBS as positive controls, chitosan-pectin-hyaluronic polyelectrolyte complex (PEC) and zinc phosphate (Zn) (a) compared to the viability of cells exposed to LH, LC3, LC6, and LC9 formulations at 50–1000 μg/ml. Error bars represent standard deviations; symbols indicate significant differences at $p < 0.05$: *compared to the negative controls (DMEM), and # in LH and LC at the same concentration, using the Student's *t*-test.

LH, the LC3, LC6, LC9 formulations and the LH solution affected HGF-1 after 24 h exposure in a dose-dependent manner (Fig. 6b). At 250–1000 μg/ml LCs, the cell viability decreased approximately 20% compared to the negative control, but at lower concentrations (50–100 μg/ml), LCs were not cytotoxic. Instead, these concentrations improved cell proliferation (Scheme 1). In contrast, 500–10 00 μg/ml LH significantly reduced the HGF-1 viability below 50% compared to the negative control ($p < 0.05$). According to ISO norms, cell viabilities above 70% indicate the compound is non-toxic or non-cytotoxic (Srivastava et al., 2018). Therefore, The LC3, LC6, LC9, and LH at a concentration below 100 μg/ml were reported as non-cytotoxic to HGF-1 cells.

Most important in developing the lidocaine hydrochloride-loaded chitosan-pectin-hyaluronic acid polyelectrolyte complex formulation is determining the ingredient that provides the most stable formulation, suitable physicochemical properties, and rapid and steady-state, controlled release with no toxicity. The formulations of 1.5% HA (LC7, LC8, LC9) demonstrated suitable physicochemical stability, even though this group demonstrated the largest particle size, zeta potential, and % EE. Moreover, the high concentration of HA provided rapid release within 5 mins and sustained release over 24 h, demonstrated no cytotoxicity to gingival fibroblasts and remained homogenous after 3 months of storage. Data such as particle size, % EE, %DL, % drug release, and cytotoxicity may inform predictions of the pharmaceutical effects and drug uptake. Therefore, PEC is not only promising vehicles in drug delivery system to transport the drug to target sites, but it also manipulated the drug by controlling the rate of drug release and prolonging the therapeutic activity primary by diffusion from the matrix mechanism (Das et al., 2011). Additional studies such as biocompatibility and therapeutic efficacy must be conducted.

Zinc sulphate (Zn), one of the metal ions, can coordinate with NH^{3+} of chitosan to form a cross-linking polyelectrolyte-metal-chelation (Wang et al., 2004; Das et al., 2011). Moreover, the advantages of adding Zn in the ternary complex system are the properties of disinfection and bactericide (Takai et al., 2002), ani-inflammation and wound healing induction (Soubhagya et al., 2020), and antimicrobial activities (Wang et al., 2003) of zinc.

First, our main objective is to design the topical pain killer formulation to treat dry socket wound as we presented a quality by designing lidocaine hydrochloride loaded in chitosan-pectin- hyaluronic acid polyelectrolyte complex which is a fast onset of action within 5 mins and continue sustained release of lidocaine for 24 h to suppress the pain from dry socket. Pathology of dry socket that is loss of blood clot in early time, exposed bone and pain induced from characteristic pain associated with dry socket have been attributed to the formation of kinins in the alveolus (Blum, 2002). The kinins activate the primary afferent nerve terminations (Blum, 2002; Cardoso et al., 2010). Treatment of dry socket in direct techniques by applying wound dressing with medication cover the exposed bone for protecting the bone from pain stimulation and lidocaine release from formulation to bare bone. According to the pathogenesis of a dry socket that the pain comes from the nerve at bone exposure site in a couple of minutes, our primary outcome is to relive such acute pain and aim to sustain release of our formation for a prolonged period until the re-epithelization or would healing process is completed. Our findings were complied with the nature of a dry socket pathogenesis, because we present a quality by design of lidocaine hydrochloride loaded in chitosan-pectin- hyaluronic acid polyelectrolyte complex which a fast onset of action within 5 mins and continue sustained release of lidocaine for 24 h to suppress the pain from dry socket. Moreover, form our formulation investigation, we found no cytotoxicity of our formulations to gingival fibroblasts, and remained homogenous after 3 months of storage. These data could be the primary outcome and could be further investigated for developing of a higher effective formulation.

It is generally known that, the effect of certain formulations in an *in vitro* study could not completely explain the effect seen in an *in vivo* setting because there are more complex factors and factors-factors interaction occurring in a living organism. Thus, to ensure the effectiveness of our developed formulations, selected formulations within a desired property (for instance, fast onset and adequate release time) should be further evaluated in an animal model. There are many models of pain assessments that have been published, for example, rats' models for orofacial pain (Martínez-García et al., 2019) and tooth extraction of rats (Cardoso et al., 2011) which might fit for our experiment and need to be considered. Thus, applying the animal models which measure the pain including pain behavior in rats' model (Damrongrungruang et al., 2020) should be further examined for convincing the clinician about the effectiveness of our formulations prior to enter clinical trial phase.

4. Conclusion

LC formulations were successfully prepared by composing of ternary polyelectrolyte complex. Concentration ratio of LH and HA was found to influence particle size, zeta potential, %EE, loading capacity, viscosity, and stability of the polyelectrolyte complex system. The LC formulation achieved prompt release (within 5 min) and demonstrated sustained drug release which cover the rapidly and continue release to provide pain reduction. LC9 presented optimum characteristics as nano-size particles, charge stability and were proved to present biocompatibility, which could potentially deliver LH for dry socket wound treatment. However, further experiments may need to investigate for its clinical efficacy.

Declaration of Competing Interest

The authors declare that they have no known competing financial interests or personal relationships that could have appeared to influence the work reported in this paper.

Acknowledgments

This project was partially supported by Research Institute of Rangsit University, Thailand (Grant no. 11/2562).

References

Archana, D., Dutta, J., Dutta, P.K., 2013. Evaluation of chitosan nano dressing for wound healing: characterization, in vitro and in vivo studies. Int. J. Biol. Macromol. 57, 193–203. https://doi.org/10.1016/j.ijbiomac.2013.03.002.

Blum, I.R., 2002. Contemporary views on dry socket (alveolar osteitis): a clinical appraisal of standardization, aetiopathogenesis and management: a critical review. Int. J. Oral Maxillofac. Surg. 31 (3), 309–317. https://doi.org/10.1054/ijom.2002.0263.

Borges, V., Maciel, V., Yoshida, C., Teixeira, T., 2015. Chitosan/pectin polyelectrolyte complex as a pH indicator. Carbohydr. Polym. 132, 537–545. https://doi.org/10.1016/j.carbpol.2015.06.047.

Bukhari, S.N.A., Roswandi, N.L., Waqas, M., Habib, H., Hussain, H., Khan, S., Sohail, M., Ramli, N.A., Thu, E.H., Hussain, Z., 2018. Hyaluronic acid, a promising skin rejuvenating biomedicine: a review of recent updates and pre-clinical and clinical investigations on cosmetic and nutricosmetic effects. Int. J. Biol. Macromol. 120, 1682–1695. https://doi.org/10.1016/j.ijbiomac.2018.09.188.

Burgoyne, C.C., Giglio, J.A., Reese, S.E., Sima, A.P., Laskin, D.M., 2010. The efficacy of a topical anesthetic gel in the relief of pain associated with localized alveolar osteitis. J. Oral Maxillofac. Surg. 68 (1), 144–148. https://doi.org/10.1016/j.joms.2009.06.033.

Cardoso, C.L., Rodrigues, M.T.V., Júnior, O.F., Garlet, G.P., de Carvalho, P.S.P., 2010. Clinical concepts of dry socket. J. Oral Maxillofac. Surg. 68 (8), 922–932. https://doi.org/10.1016/j.joms.2009.09.085.

Cardoso, C.L., Ferreira Júnior, O., Carvalho, P.S.P.d., Dionísio, T.J., Cestari, T.M., Garlet, G.P., 2011. Experimental dry socket. Microscopic and molecular evaluation of two treatment modalities. Acta. Cir. Bras. 26 (5), 365–372. https://doi.org/10.1590/S0102-86502011000500007.

da Silva, J., Ferreira, S., Reis, A., Cook, M., Bruschi, M.L., 2018. Assessing mucoadhesion in polymer gels: the effect of method type and instrument variables. Polymers. 10, 1–19. https://doi.org/10.3390/polym10030254.

Dahiya, P., Kamal, R., 2014. Hyaluronic acid: a boon in periodontal therapy. North Am. J. Med. Sci. 5, 309–315. https://doi.org/10.4103/1947-2714.112473.

Damrongrungruang, T., Panpitakkul, P., Somudorn, J., Sangchart, P., Mahakunakorn, P., Uthaiwat, P., Daduang, J., Panyatip, P., Puthongking, P., Priprem, A., 2020. Glutaryl melatonin niosome gel for topical oral mucositis: anti- inflammatory and anticandidiasis. Curr. Drug Deliv. 17 (3), 195–206. https://doi.org/10.2174/1567201817666200122162545.

Das, S., Chaudhury, A., Ng, K.Y., 2011. Preparation and evaluation of zinc–pectin–chitosan composite particles for drug delivery to the colon: role of chitosan in modifying in vitro and in vivo drug release. Int. J. Pharm. 406 (1–2), 11–20. https://doi.org/10.1016/j.ijpharm.2010.12.015.

Deed, R., Ooney, P., Umar, P., Orton, J., Mith, J., Freemont, A., Kumar, S., 1997. Early-response gene signaling is induced by angiogenic oligosaccharides of hyaluronic in endothelial cells. Inhibit by non-angiogenic, high-molecular-weight hyaluronan. Int. J. Cancer 71, 251–256.

Folchman-Wagner, Z., Zaro, J., Shen, W.C., 2017. Characterization of polyelectrolyte complex formation between anionic and cationic poly(amino acids) and their potential applications in pH-dependent drug delivery. Molecules 22, 1–14. https://doi.org/10.3390/molecules22071089.

Garg, A., Garg, N., Kaur, D., Sharma, S., Tahun, I.A., Kumar, R., 2016. Evaluation of efficacy of 2% lidocaine gel and 20% benzocaine gel for topical anesthesia. Endodontology 28, 38–41. https://doi.org/10.4103/0970-7212.184338.

Gennari, A., de la Rosa, J., Hohn, E., Pelliccia, M., Lallana, E., Donno, R., Tirella, A., Tirelli, N., 2019. The different ways to chitosan/hyaluronic acid nanoparticles: templated vs direct complexation. Influence of particle preparation on morphology, cell uptake and silencing efficiency. Beilstein J. Nanotechnol. 10, 2594–2608. https://doi.org/10.3762/bjnano.10.250.

Genovese, D., Lozano, J., 2006. Contribution of colloidal forces to the viscosity and stability of cloudy apple juice. Food Hydrocoll. 20 (6), 767–773. https://doi.org/10.1016/j.foodhyd.2005.07.003.

Graça, A., Gonçalves, L., Raposo, S., Ribeiro, H., Marto, J., 2018. Useful in vitro techniques to evaluate the mucoadhesive properties of hyaluronic acid-based ocular delivery systems. Pharmaceutics 10, 110–111. https://doi.org/10.3390/pharmaceutics10030110.

Hong, W.G., Jeong, G.W., Nah, J.W., 2018. Evaluation of hyaluronic acid-combined ternary complexes for serum-resistant and targeted gene delivery system. Int. J. Biol. Macromol. 115, 459–468. https://doi.org/10.1016/j.ijbiomac.2018.04.053.

Ishihara, M., Kishimoto, S., Nakamura, S., Sato, Y., Hattori, H., 2019. Polyelectrolyte complexes of natural polymers and their biomedical applications 672, 1–12 Polymers. 11 (4). https://doi.org/10.3390/polym11040672.

Kamal, A., Salman, B., Abdul Razak, N.H., Qabbani, A.A., Samsudin, A.R., 2020. The efficacy of concentrated growth factor in the healing of alveolar osteitis: a clinical study. Int. J. Dent. 2020, 1–9. https://doi.org/10.1155/2020/9038629.

Lee, H., 2016. Recent advances in topical anesthesia. J. Dent. Anesth. Pain Med. 16, 237–244 https://doi.org/10.17245/jdapm.2016.16.4.237.

Lee, J.K., 1998. Surface charge effects on particulate retention by microporous membrane filters in liquid filtration. Environ. Eng. Res. 3 (2), 97–104.

Limsitthichaikoon, S., Sinsuebpol, C., 2019. Electrostatic effects of metronidazole loaded in chitosan-pectin polyelectrolyte complexes. Key Eng. Mater. 819, 27–32 https://doi:10.4028/www.scientific.net/KEM.819.27.

López-Esparza, R., Balderas Altamirano, M.A., Pérez, E., Gama Goicochea, A., 2015. Importance of molecular interactions in colloidal dispersions. Adv. Condens. Matter Phys. 2015, 1–8. https://doi.org/10.1155/2015/683716.

Maciel, V.B.V., Yoshida, C.M.P., Franco, T.T., 2015. Chitosan/pectin polyelectrolyte complex as a pH indicator. Carbohydr. Polym. 132, 537–545. https://doi.org/10.1016/j.carbpol.2015.06.047.

Marudova, M., MacDougall, A.J., Ring, S.G., 2004. Pectin-chitosan interactions and gel formation. Carbohydr. Res. 339 (11), 1933–1939. https://doi.org/10.1016/j.carres.2004.05.017.

Martínez-García, M.A., Migueláñez-Medrán, B.C., Goicoechea, C., 2019. Animal models in the study and treatment of orofacial pain. J. Clin. Exp. Dent. 11 (4), e382–e390. https://doi.org/10.4317/jced.55429.

Metin, M., Tek, M., Sener, I., 2006. Comparison of two chlorhexidine rinse protocols on the incidence of alveolar osteitis following the surgical removal of impacted third molars. J. Contemp. Dent. Pract. 7 (2), 79–86.

Mhlanga, N., Ray, S.S., 2015. Kinetic models for the release of the anticancer drug doxorubicin from biodegradable polylactide/metal oxide-based hybrids. Int. J. Biol. Macromol. 72, 1301–1307. https://doi.org/10.1016/j.ijbiomac.2014.10.038.

Mitrevej, A., Sinchaipanid, N., Rungvejhavuttivittaya, Y., Kositchaiyong, V., 2001. Multiunit controlled-release diclofenac sodium capsules using complex of chitosan with sodium alginate or pectin. Pharm. Dev. Technol. 6 (3), 385–392. https://doi.org/10.1081/PDT-100002.

Naidu, V., Madhusudhana, K., Sashidhar, R., Ramakrishna, S., Khar, R., Ahmed, F., Diwan, P., 2009. Polyelectrolyte complexes of gum kondagogu and chitosan, as diclofenac carriers. Carbohydr. Polym. 76 (3), 464–471. https://doi.org/10.1016/j.carbpol.2008.11.010.

Nath, S.D., Abueva, C., Kim, B., Lee, B.T., 2015. Chitosan–hyaluronic acid polyelectrolyte complex scaffold crosslinked with genipin for immobilization and controlled release of BMP-2. Carbohydr. Polym. 115, 160–169. https://doi.org/10.1016/j.carbpol.2014.08.077.

Ostolska, I., Wiśniewska, M., 2014. Application of the zeta potential measurements to explanation of colloidal Cr_2O_3 stability mechanism in the presence of the ionic polyamino acids. Colloid Polym. Sci. 292 (10), 2453–2464. https://doi.org/10.1007/s00396-014-3276-y.

Pandey, S., Mishra, A., Raval, P., Patel, H., Gupta, A., Shah, D., 2013. Chitosan-pectin polyelectrolyte complex as a carrier for colon targeted drug delivery. J. Young Pharm. 5 (4), 160–166. https://doi.org/10.1016/j.jyp.2013.11.002.

Potaś, J., Szymańska, E., Winnicka, K., 2020. Challenges in developing of chitosan – based polyelectrolyte complexes as a platform for mucosal and skin drug delivery. Eur. Polym. J. 140 (5), 110020. https://doi.org/10.1016/j.eurpolymj.2020.110020.

Priftis, D., Xia, X., Margossian, K.O., Perry, S.L., Leon, L., Qin, J., de Pablo, J.J., Tirrell, M., 2014. Ternary, tunable polyelectrolyte complex fluids driven by complex coacervation. Macromolecules 47 (9), 3076–3085. https://doi.org/10.1021/ma500245j.

Raoufi, N., Fang, Y., Kadkhodaee, R., Phillips, G.O., Najafi, M.N., 2017. Changes in turbidity, zeta potential and precipitation yield induced by Persian gum-whey protein isolate interactions during acidification. J. Food Process. Preserv. 41 (3), e12975. https://doi.org/10.1111/jfpp.2017.41.issue-310.1111/jfpp.12975.

Sherman, P., 1970. Rheology of dispersed systems. In: Industrial Rheology. Academic Press, London, pp. 97–183.

Shevel, E., 2018. Painful dry socket: an alternative perspective. S. Afr. Dent. J. 73, 456–458 https://doi.org/10.17159/2519-0105/2018/v73no7a5.

Srivastava, G.K., Alonso-Alonso, M.L., Fernandez-Bueno, I., Garcia-Gutierrez, M.T., Rull, F., Medina, J., Coco, R.M., Pastor, J.C., 2018. Comparison between direct contact and extract exposure methods for PFO cytotoxicity evaluation. Sci. Rep. 8 (1). https://doi.org/10.1038/s41598-018-19428-5.

Soubhagya, A.S., Moorthi, A., Prabaharan, M., 2020. Preparation and characterization of chitosan/pectin/ZnO porous films for wound healing. Int. J. Biol. Macromol. 157, 135–145. https://doi.org/10.1016/j.ijbiomac.2020.04.156.

Swain, G.P., Patel, S., Gandhi, J., Shah, P., 2019. Development of Moxifloxacin Hydrochloride loaded in-situ gel for the treatment of periodontitis: In-vitro drug release study and antibacterial Activity. J. Oral Biol. Craniofac. Res. 9 (3), 190–200. https://doi.org/10.1016/j.jobcr.2019.04.001.

Takai, K., Ohtsuka, T., Senda, Y., Nakao, M., Yamamoto, K., Matsuoka, J., Hirai, Y., 2002. Antibacterial properties of antimicrobial-finished textile products. Med. Microbiol. Immunol. 46 (2), 75–81. https://doi.org/10.1111/mim.2002.46.issue-210.1111/j.1348-0421.2002.tb02661.x.

Tarakji, B., Saleh, L., Umair, A., Azzeghaiby, S., Hanouneh, S., 2015. Systemic review of dry socket: aetiology, treatment, and prevention ZE10–ZE13 J. clin. diagn. res. 9 (4). https://doi.org/10.7860/JCDR/2015/12422.5840.

Veale, B., 2015. Alveolar osteitis: a critical review of the aetiology and management. Oral Surg. 8 (2), 68–77. https://doi.org/10.1111/ors.2015.8.issue-210.1111/ors.12130.

Wang, X., Du, Y., Liu, H., 2003. Preparation, characterization and antimicrobial activity of chitosan-Zn complex. Carbohydr. Polym. 56 (1), 21–26. https://doi.org/10.1016/j.carbpol.2003.11.007.

Wang, H., Yang, B., Sun, H., 2017. Pectin-Chitosan polyelectrolyte complex nanoparticles for encapsulation and controlled release of nisin. Am. J. Polym. Sci. Tech. 3, 82–88 https://doi.org/10.11648/j.ajpst.20170305.11.

Wang, X., Du, Y., Liu, H., 2004. Preparation, characterization and antimicrobial activity of chitosan-Zn complex. Carbohydr. Polym. 56 (1), 21–26. https://doi.org/10.1016/j.carbpol.2003.11.007.

Zhang, L., Wang, J., Ni, C., Zhang, Y., Shi, G., 2016. Preparation of polyelectrolyte complex nanoparticles of chitosan and poly(2-acry1amido-2-methylpropanesulfonic acid) for doxorubicin release. Mater. Sci. Eng., C 58 (1), 724–729. https://doi.org/10.1016/j.msec.2015.09.044.